The *Saccharomyces cerevisiae* Linker Histone Hho1p, with Two Globular Domains, Can Simultaneously Bind to Two Four-Way Junction DNA Molecules†

Georgia Schäfer,‡ Elizabeth M. Smith,‡ and Hugh G. Patterton*

Department of Biotechnology, University of the Free State, P.O. Box 339, Bloemfontein, 9300 South Africa

Received June 20, 2005; Revised Manuscript Received October 20, 2005

ABSTRACT: *Saccharomyces cerevisiae* encodes a single linker histone, Hho1p, with two globular domains. This raised the possibility that Hho1p could bind to two nucleosome cores simultaneously. To evaluate this idea, we studied the ability of a four-way junction, immobilized on the surface of a magnetic bead, to pull down a radiolabeled four-way junction in the presence of different Hho1 proteins. Four-way junctions are known to bind to H1, presumably due to structure similarities to the DNA at the nucleosomal entry/exit point. We found a significant increase in the ability of full-length Hho1p to pull down radiolabeled four-way junction DNA under ionic conditions where both globular domains could bind. The binding was structure specific, since the use of double-stranded DNA, or a mutant Hho1p in which the second DNA binding site of globular domain 1 was abolished, resulted in a significant decrease in bridged binding. Additionally, bridged binding required a covalent attachment between the two globular domains, since factor Xa protease treatment of the complex formed by a modified Hho1p that contained a factor Xa cleavage site between the two globular domains resulted in a significant release of radiolabeled four-way junction. These findings demonstrated that the two globular domains independently associated with two different four-way junction molecules in a manner that required amino acid residues implicated in structure-specific binding in the nucleosome. We discuss the implication of these findings on the chromatin structure of yeast and propose a model where a single Hho1 protein binds to two serially adjacent nucleosomes.

Chromatin is composed of arrays of nucleosomes, where each nucleosome contains an octamer that is formed by two copies of the H2A−H2B and of the H3−H4 heterodimers that are symmetrically located relative to a pseudo-2-fold symmetry axis. The H3−H4 dimers interact via a four-helix bundle at the H3 C-termini, and the H2A−H2B dimers bind to the resulting central H3−H4 tetramer via a similar four-helix bundle interaction between the H2B and H4 C-termini (*1*). Approximately 166 bp of duplex DNA is wound onto the histone octamer as two turns of a negative superhelix (*2*). A single copy of the linker histone H1 binds between the superhelical gyres on the side of DNA entry and exit, close to the pseudodyad axis (*3*).

The H1 histones form a large family of proteins. In mammals, eight isotypes have been identified, including five somatic isotypes (H1a−e), a testis-specific H1t, an oocyte specific H1oo, and H1°, a replacement variant associated with terminally differentiated cell types, related to H5, which is found in nucleated avian erythrocytes (*4*). The canonical metazoan H1 protein contains a globular domain flanked by variable N-terminal and C-terminal regions. Some lower eukaryotes have atypical linker histones, such as *Tetrahymena*, where the linker histones resembled an isolated C-terminal tail (*5*), or *Saccharomyces cerevisiae*, where the H1 molecule contained two globular domains (*6*, *7*).

X-ray crystallographic and NMR studies of H1 (*8*), H5 (*9*), and the isolated globular domains of *S. cerevisiae* Hho1p (*7*, *10*) showed that the globular domain assumed a single-winged helix conformation, composed of three α-helices and a C-terminal *β*-hairpin. Two clusters of basic amino acid residues were identified on opposite sides of the globular domain (*8*, *9*, *11*) and were shown to be required for the proper binding of the H5 globular domain to a nucleosome (*12*). The globular domain of H5 was located between the two superhelical gyres on the nucleosome, where the two identified basic clusters could contact the DNA in the terminal helical turn and the DNA backbone enclosing the minor groove at the pseudo-2-fold axis (*3*), respectively.

Compared to the globular domain, the N-terminal and C-terminal regions of H1 displayed low sequence complexity (*13*). The C-terminal domain was particularly rich in the amino acids P, A, and K and generally contained several repeats of the consensus S/TPKK motif or variations thereof (*14*). Although the N-terminal and C-terminal tails of H1 were normally unstructured in aqueous solution, sequence patterns suggestive of a structural motif were reported for the C-terminal tail (*15*), and this tail was shown to assume a significant α-helical character in the presence of tetrahedral anions (*16*) or when bound to DNA (*17*, *18*).

Histone H1 was further shown to be required for the salt-dependent condensation of mixed sequence nucleosomal

† This work was supported by the Wellcome Trust (H.G.P. was a Wellcome Trust International Senior Research Fellow in Biomedical Science in South Africa) and the National Research Foundation (Grant FA2004041900042 to H.G.P.). G.S. was the recipient of postdoctoral fellowships from the NRF and German Academic Exchange Service (DAAD), and E.M.S. received a postgraduate bursary from the NRF.

* To whom correspondence should be addressed. Telephone: 27 51 4012274. Facsimile: 27 51 4019376. E-mail: patterh.sci@mail.uovs.ac.za.

‡ Present address: Institute for Infectious Diseases and Molecular Medicine, University of Cape Town, Rondebosch, South Africa.

10.1021/bi0511787 CCC: $30.25
Published on Web 11/23/2005

Table 1: Oligonucleotide Primers Used in This Study

oligonucleotide primer	nucleotide sequence
GD1-F	GGGCGCCATGTCCAAGAGTTACAGGGAGTT
GD1-R	GGGCTCGAGTCATTTCTTCTTGGCCAGTT
GD2-F	GGGGCGCCATGGCCTCTTCGCCTTCTTCA
GD2-R	GGGGCTCGAGTCATTTGACCTTCTTCTTG
HHO1-F	GGGTGATCATTGAAGGGCTC
HHO1-R	GGGAGGCCTTCTTGGCGGTA
HHO1-FXa-F	ACGAAGCTAATCGAAGGTCGTGCGCCAAAG
HHO1-FXa-R	CTTTGGCGCACGACCTTCGATTAGCTTCGT
HHO1-GD1-F	CGGGCTTTGTTAGCAGCCGG
HHO1-GD1-R	TGTTTAACTTTAAGAAGGAG
HHO1-GD1-R40E-K42E-F	CGACTGGATCCCTTTTCTTCTTCCAAAGCCGTGAGCCCTTC
HHO1-GD1-R40E-K42E-R	GAAGGGCTCACGGCTTTGGAAGAAGAAAAGGGATCCAGTCG
HHO1-GD1-K52A-F	TTTTCCTTGATAAAAGCCTTGAGTGCCGGAC
HHO1-GD1-K52A-R	GTCCGGCACTCAAGGCTTTTATCAAGGAAAAC
HHO1-GD1-K92A-F	GATTTCTTCTTGGCCAGAGCCACAGCACCAGC
HHO1-GD1-K92A-R	GCTGGTGCTGTGGCTCTGGCCAAGAAGAAATC

arrays into a regular chromatin fiber (*19*). Although the arrangement of nucleosomes in the 30 nm fiber is not currently well described, there is experimental support for a two-start helical arrangement with the linker DNA connecting serial nucleosome neighbors through the fiber center (*19*−*21*). Interestingly, Gould and colleagues reported that the compaction of native, mixed-sequence nucleosome arrays required core histone tails in addition to a linker histone (*22*), a finding also reported by the Hansen laboratory (*23*). Notably, the N-terminal tail of histone H4, previously found to contact an acidic patch on the H2A−H2B dimer of a different nucleosome in the crystal (*1*), exhibited the greatest effect on compaction of tandem nucleosome arrays in the absence of a linker histone (*24*). The ability of the linker histone to facilitate chromatin folding was conferred by the lysine-rich C-terminal tail (*22*, *25*). It therefore appeared likely that the linker histone globular domain acted as a "structure recognition module", placing the lysine-rich C-terminal tail at a location in the nucleosome where it assumed a helical character when associated with the linker DNA and effected partial charge neutralization of the DNA that connected adjacent nucleosomes. This partial neutralization was proposed to stabilize the 30 nm fiber.

The study of chromatin in *S. cerevisiae* has contributed significantly to our understanding of the role of chromatin structure in the regulation of the genetic functions and processes involving the DNA molecule. The covalent modifications of the core histone tails and histone fold domains, ATP-dependent chromatin remodelers, and histone variant swapping presented chromatin as a complex that both dynamically responded to local DNA activities and modulated these activities by dynamic changes in its structural properties. To extend this understanding of the regulation of DNA function in *S. cerevisiae* to include higher order chromatin structures, in particular, the role and the regulation of chromatin condensation, requires a firm biochemical grasp of the manner in which linker histone Hho1p binds to chromatin. Since yeast Hho1p was unusual in that it contained two globular domains, we were interested in understanding the binding mode of this protein in chromatin. Although both globular domains could bind to DNA independently under different conditions (*26*), it is not known whether the intact, full-length Hho1p could bind to two nucleosome cores at the same time. Here we investigated the ability of Hho1p to simultaneously bind to two four-way junction molecules as a model for two nucleosome cores. We interpret our data in terms of possible structures for higher order folded forms of chromatin in *S. cerevisiae*.

EXPERIMENTAL PROCEDURES

Plasmid Construction. Standard molecular biological techniques used were as described (*27*), and enzymes were used as recommended by the respective manufacturers. An expression plasmid containing the coding sequence of globular domain 1 (GD1)[1] was constructed by ligation of a *Sfo*I/*Xho*I digested fragment, produced by a polymerase chain reaction (PCR) with Pfu DNA polymerase (Promega) using the *HHO1* ORF-containing plasmid pRS413-*HHO1* (*11*) as template, and the oligonucleotide primers GD1-F and GD1-R (Table 1), into appropriately restricted pProEx A plasmid (Novagen). The coding sequence of globular domain 2 (GD2), produced by PCR with the GD2-F and GD2-R oligonucleotide primers (Table 1), was similarly restricted with *Sfo*I/*Xho*I and ligated into pProEx A. The plasmids were denoted pProEx A-GD1 and pProEx A-GD2, and placed an in-frame 6 × His sequence N-terminal to the inserted coding sequences.

Construction of the Hho1p expressing pET20b(+)-HHO1 plasmid was previously described (*11*). A construct encoding a Hho1 protein containing a factor Xa cleavage site between the two globular domains was produced by using a two-step template mismatched PCR method (*28*), with Pfu DNA polymerase and the oligonucleotide primer pairs HHO1-R/HHO1-Fxa-R and HHO1-Fxa-F/HHO1-R (Table 1). The recovered full-length fragment was digested with *Bcl*I and *Stu*I and ligated into the similarly cleaved pET20b(+) vector (Novagen) containing a C-terminal 6 × His sequence. This procedure introduced the amino acid sequence IEGR C-terminal to L154 in the protein.

A construct encoding the full-length Hho1p with K59E, R61E, K71A, and K114A substitution mutations (corresponding to the K40, R42, K52, and K95 residues of the second DNA binding site of histone H5) was produced by a

[1] Abbreviations: GD1, globular domain 1; GD2, globular domain 2; PCR, polymerase chain reaction; SDS, sodium dodecyl sulfate; PAGE, polyacrylamide gel electrophoresis; EDTA, ethylenediaminetetraacetic acid; PMSF, phenylmethanesulfonyl fluoride; MALDI-TOF, matrix-assisted laser desorption ionization/time of flight; 4WJ, four-way junction.

series of template-mismatched procedures. An initial PCR was performed to introduce the K59E, R61E, and K71A substitution mutations using the complementary, HPLC-purified primer pair HHO1-GD1-R40E-K42E-K52A-F and HHO1-GD1-R40E-K42E-K52A-R. Methylated template DNA was digested in the recovered amplified product by *Dpn*I (Promega) cleavage, and the amplified fragment was transformed into XL1-Blue cells. Plasmid was isolated from the bacterial cells and used as a template for a second PCR procedure using the primer pair HHO1-GD1-K92A-F and HHO1-GD1-K92A-R. The modified PCR product was again enriched by *Dpn*I cleavage and transformed into XL1-Blue. The isolated plasmid was digested with *Nde*I/*Xho*I and ligated into similarly digested pET20b(+) and denoted pET20b(+)-HHO1-mut.

All ligation mixes were initially transformed by electroporation with a Micropulser (Bio-Rad) into *Escherichia coli* strain DH5α (Invitrogen), and the recovered plasmids were verified by restriction enzyme digestion and partial nucleotide sequencing and subsequently transformed into BL21(DE3) pLysS (Promega) for overexpression.

Protein Overexpression and Purification. A 5 mL overnight culture of BL21(DE3) pLysS containing the appropriate pET-20b(+) plasmid (encoding the Hho1, Hho1-FXa, or Hho1-mut proteins) or the pProEx A plasmid (encoding the GD1 or GD2 proteins) was prepared in LB medium [10 g of tryptone (Becton Dickinson), 5 g of yeast extract (Becton Dickinson), and 10 g of NaCl] supplemented with ampicillin (50 μg/mL) and chloramphenicol (34 μg/mL). This culture was inoculated into 1 L of LB medium with antibiotics and incubated at 37 °C with orbital shaking (300 rpm) to an OD_{600} of 0.3−0.4, and expression was then induced with 0.4 mM isopropyl β-D-thiogalactopyranoside (USB). Induction was allowed for 2 h at 37 °C with orbital shaking (300 rpm), and cells were harvested by centrifugation (10000*g*, 20 min, 4 °C) and resuspended in 20 mL of binding buffer (5 mM imidazole, 500 mM NaCl, 20 mM Tris-HCl, pH 7.9). All buffers used for the loading, washing, and elution of GD2 from the subsequent nickel agarose column were adjusted to 100 mM sodium phosphate to improve GD2 yield. Cells were ruptured by sonication for 60 cycles, each composed of 45 s of sonication on ice followed by 15 s incubation on ice, using a 0.4 cm tip and an intensity setting of 30 (Bronwill Biosonik III sonicator; Bronwill Scientific). The cell debris was removed by centrifugation (39000*g*, 20 min, 4 °C), the supernatant was applied to a His Bind nickel agarose column (Novagen), and the proteins were eluted from the column using the manufacturer's protocol. Fractions containing the desired protein were identified by SDS−PAGE, pooled, and dialyzed overnight at 4 °C against loading buffer (100 mM potassium phosphate, 1 mM EDTA, pH 7.2).

Protein samples were further purified on a 0.5 mL bed volume of Bio-Rex 70 (Bio-Rad), eluted with a 1 mL linear gradient of 10−50% (w/v) guanidine hydrochloride in loading buffer. Protein fractions were pooled, dialyzed overnight at 4 °C against 1 mM Tris-HCl, pH 7.4, 1 mM EDTA, and 0.1 mM PMSF, and stored at −20 °C. The identities of some of the purified recombinant proteins were confirmed by matrix-assisted laser desorption ionization/time-of-flight (MALDI-TOF) mass spectrometry of partial tryptic digests as previously described (*29*). Protein concentrations were determined by a Bradford assay (Bio-Rad) using BSA as standard.

Gel Shifts. Four 30 bp oligonucleotides (*30*) were ^{32}P-labeled at the 5′ ends and annealed as described (*31*) to form four-way junction (4WJ) DNA. The indicated amounts of protein (Hho1, Hho1-FXa, Hho1-mut, GD1, or GD2) were incubated with 5 nM labeled 4WJ DNA in 20 μL of gel shift binding buffer [10 mM Tris-HCl, pH 7.4, 50 mM NaCl, 10% (v/v) glycerol, 100 μg/mL BSA, 1 mM dithiothreitol, 50 ng/mL sonicated salmon sperm DNA (Sigma-Aldrich)], containing the sodium phosphate concentrations indicated in the text, at room temperature for 10 min followed by incubation on ice for 15 min. DNA−protein complexes were then analyzed on preelectrophoresed (100 V, 2 h, 4 °C) 6% (w/v) polyacrylamide [60:1 (w/w) acrylamide:bisacrylamide (Bio-Rad)] gels in 0.5 × TBE (50 mM Tris-HCl, 50 mM boric acid, 2 mM EDTA). Electrophoresis was carried out at 4 °C for 3 h at 250 V, and the gels were dried, exposed overnight to a storage phosphor screen (Kodak), and visualized in a phosphoimager (Personal Molecular Imager FX; Bio-Rad).

Magnetic Pull Down of Biotin-Labeled 4WJ DNA. Biotin-labeled 4WJ DNA was prepared as described (*31*) using a strand 1 oligonucleotide (*30*) synthesized with a 5′-biotinylated nucleotide. A volume of 20 μL (0.2 mg) of streptavidin-coated magnetic beads (Roche), washed three times in TEN_{100} (10 mM Tris-HCl, pH 7.5, 1 mM EDTA, 100 mM NaCl), was incubated with a large molar excess (5 nM) of biotin-labeled 4WJ DNA or double-stranded DNA for 30 min at room temperature. Particles were washed twice in TEN_{1000} (10 mM Tris-HCl, pH 7.5, 1 mM EDTA, 1 M NaCl), equilibrated in gel shift binding buffer 1 containing the concentrations of sodium phosphate indicated, and incubated with the indicated concentrations of protein for 10 min at room temperature, followed by 15 min incubation on ice. Samples were then equilibrated in gel shift binding buffer 2 containing the indicated concentrations of sodium phosphate and incubated with 5 nM ^{32}P-labeled 4WJ DNA on ice for 20 min. The magnetic beads were collected with a particle separator (Roche), and label associated with the supernatants and pellet was quantitated by liquid scintillation counting.

RESULTS

To determine whether the linker histone Hho1p from *S. cerevisiae*, which contains two separate globular domains (*6*, *26*), could bind to two different nucleosome cores simultaneously, we studied the interaction of various full-length Hho1p and globular domain peptides with four-way DNA junctions. It was previously shown that the linker histone H1 formed a specific complex with 4WJ DNA, presumably due to the structural similarities between the 4WJ DNA and the DNA at the entry/exit point of the nucleosome core (*32*, *33*).

Both GD1 and GD2 Formed Stable Binary Complexes with 4WJ DNA. We were interested in assessing the ability of a single Hho1p molecule to bind in a bridged manner between two separate 4WJ molecules. It was a concern that the binding of one globular domain of Hho1p to a 4WJ would result in the binding of the second globular domain to a second site on the same 4WJ molecule due to local

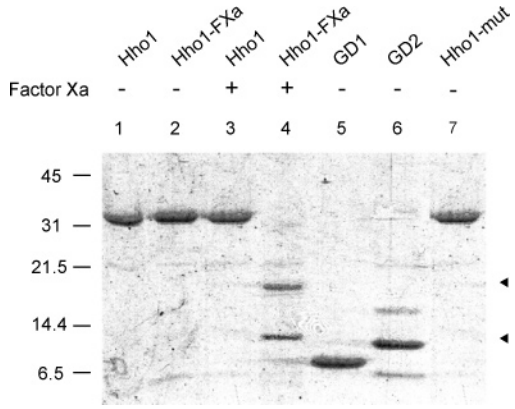

FIGURE 1: Purification of the full-length native and modified Hho1 proteins and globular domain 1 and 2 peptides. Recombinant full-length yeast linker histone Hho1p (lanes 1 and 3), a modified Hho1p protein containing a factor Xa cleavage site C-terminal to L154 (Hho1-FXa, lanes 2 and 4), GD1 (lane 5), GD2 (lane 6), and a modified Hho1p protein with K59E, R61E, K71A, and K114A substitution mutations (Hho1-mut, lane 7) were overexpressed and isolated from bacterial cultures. To assess the ability of factor Xa to cleave the modified Hho1 protein, Hho1p and Hho1-FXa protein were incubated in the absence (lanes 1 and 3) or presence (lanes 2 and 4) of factor Xa. The arrowheads indicate the position of the two peptide fragments resulting from the factor Xa cleavage of the Hho1-FXa protein.

concentration effects, thereby limiting bridged binding to two separate 4WJ molecules. To avoid this possibility, we sought ionic conditions that allowed the binding of only the one and not the other globular domain to a 4WJ molecule. The aim was to allow binding of only the one globular domain to a 4WJ molecule, adjustment of the ionic strength, and the subsequent binding of the second globular domain to a different 4WJ molecule. To test this approach, peptides that corresponded to globular domain 1 (GD1) and globular domain 2 (GD2), as well as full-length native Hho1p, full-length Hho1p in which the second DNA binding site of GD1 was abolished (Hho1-mut), and Hho1p that contained a factor Xa cleavage site in the region between the two globular domains (Hho1-FXa), were overexpressed in *E. coli* and purified (Figure 1). Gel-shift analysis suggested that the minor contaminating bands visible in the GD2 preparation (lane 6, Figure 1) did not bind to 4WJ DNA and were therefore not expected to interfere with the analysis. The presence of the His tag in the protein, similarly, did not have a detectable influence on DNA binding, as confirmed by gel-shift analysis of intact peptides and peptides in which the His tag was removed by protease cleavage (data not shown).

The binding of GD1 and GD2 to 4WJ DNA was studied by mixing different concentrations of GD1 or GD2 with radiolabeled 4WJ DNA and electrophoretically resolving the complexes formed in native polyacrylamide gels. The appearance of a sharp band of reduced mobility is generally regarded as due to the formation of a specific complex between the protein and the 4WJ DNA (*33*). Both GD1 and GD2 formed stable binary complexes with 4WJ DNA (Figure 2), although the apparent affinity of the two globular domains for 4WJ DNA differed, in agreement with the recent report by Thomas and colleagues (*26*). Approximately equal amounts of radiolabel appeared in the retarded binary complex and the free 4WJ DNA (50% shift) at 4 μM peptide for GD1 (lane 5 of Figure 2A), whereas GD2 produced a 50% shift at 0.1 μM GD2 (lane 9 of Figure 2B). Since the

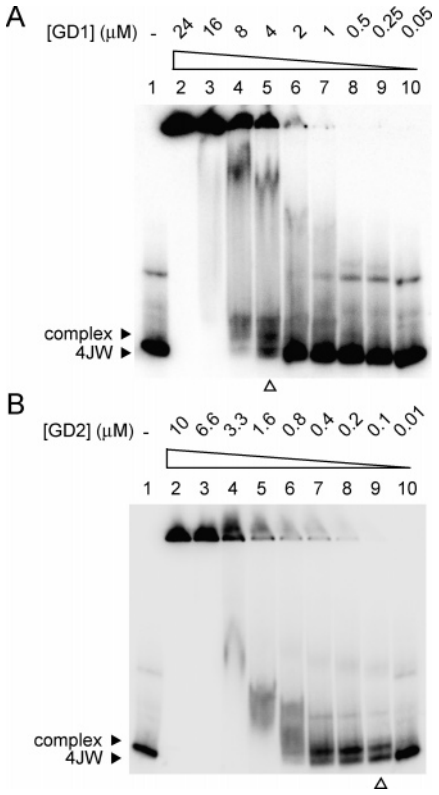

FIGURE 2: Binding of GD1 and GD2 to 4WJ DNA. Aliquots of 5 nM of radiolabeled 4WJ DNA were incubated with the indicated amounts of (A) GD1 (lanes 1−10) or (B) GD2 (lanes 1−10) and resolved on a 6% polyacrylamide gel. The phosphorimage is shown. The bands corresponding to free 4WJ DNA or the binary complex are indicated to the left, and the lanes with approximately equal amounts of free 4WJ DNA and binary complex (50% shift) are identified by the white triangles to the bottom.

concentration of the two globular domains would be identical in an intact Hho1p molecule, we next investigated the effect of phosphate concentration on the binding of GD1 and GD2 to 4WJ DNA at 4 μM peptide, the concentration that was required to produce a 50% shift with GD1, the peptide with lower apparent affinity. We chose sodium phosphate, since this salt was shown to efficiently disrupt H1−DNA associations, and the tetrahedral phosphate ion was also shown to facilitate folding of linker histone globular domains (*7*). It was previously shown that the 4WJ DNA was in rapid equilibrium between the various X-stacked and the planar conformations in the range of ionic conditions employed in this study (*34*). It was therefore expected that the structure(s) that was (were) preferentially bound by the globular domain of the linker histone would be readily present as a species in this dynamic equilibrium.

There Is Significant Binding of GD2, but Not of GD1, to 4WJ DNA at 100 mM Phosphate. The binary complex formed by GD1 and 4WJ DNA in the absence of added phosphate (0 mM) was significantly destabilized by an increase in phosphate concentration (Figure 3). In contrast, in the absence of phosphate ion, GD2 produced an aggregate that did not enter the gel matrix (Figure 3), and a binary complex only became detectable at phosphate concentrations in excess of 150 mM (Figure 3). This result demonstrated a clear difference in the apparent affinity of GD1 and GD2 for 4WJ DNA that could be modulated by the phosphate concentration. In particular, it showed that at 4 μM concen-

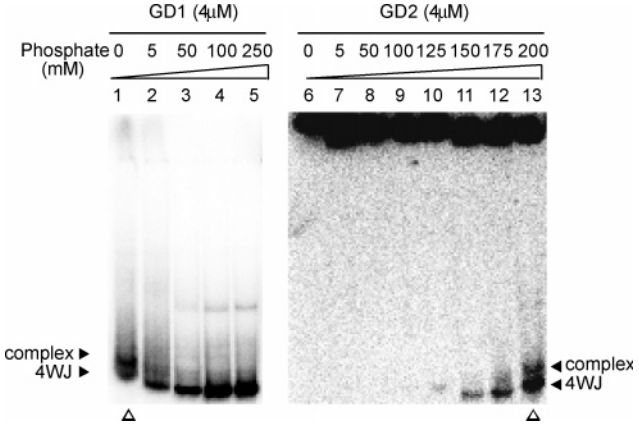

FIGURE 3: Effect of sodium phosphate on the binding of GD1 and GD2 to 4WJ DNA. Radiolabeled 4WJ DNA (5 nM) was incubated with 4 μM GD1 (lanes 1−5) or GD2 (lanes 6−13) in the presence of the indicated amounts of added sodium phosphate and electrophoresed and visualized as in Figure 2. The bands corresponding to free 4WJ DNA or the binary complex are indicated on the sides, and the lanes exhibiting approximately 50% shift are identified by the white triangles to the bottom.

trations GD2 bound to 4WJ DNA in the presence of 100 mM phosphate, whereas GD1 did not.

We next studied the effect of phosphate ion on the binding of full-length Hho1p to 4WJ DNA. It was found that at 0 mM phosphate, in contrast to the results with the globular domain peptides, a binary complex only became detectable at Hho1p concentrations of 0.05−0.1 μM (lanes 6 and 7, Figure 4A). Phosphate also destabilized the Hho1p complex, since a shifted band corresponding to Hho1p bound to 4WJ DNA only became readily detectable at a Hho1p concentration of 0.2 μM at 100 mM phosphate ion (lane 5, Figure 4B). Since 0.1 μM was the highest concentration of Hho1p that produced a binary complex with limited aggregation in the absence of the tetrahedral ion (Figure 4A), it was decided to use this concentration of Hho1p for the bridged binding studies reported below. The gel-shift behavior of the Hho1-FXa protein was identical to that of Hho1p (data not shown).

The Bridged Binding Assay Mimics the Binding Behavior of the Globular Domains Determined by Electrophoresis. We wanted to assess the ability of full-length Hho1p to simultaneously bind to two separate 4WJ molecules in a bridged fashion. This involved immobilizing a biotin-tagged 4WJ DNA on a streptavidin-coated magnetic bead and determining the amount of radiolabeled 4WJ DNA that could be pulled down in the presence of Hho1p. The general experimental scheme is shown in Figure 5. It was previously shown that the presence of a terminal biotin moiety did not limit the conformational freedom of a 4WJ molecule (*34*), and it was therefore not expected to influence protein binding.

To determine the possible contribution of nonspecific binding in this experimental approach, we first studied the binding behavior of the isolated globular domains. When 4 μM GD1 or GD2 and the radiolabeled 4WJ DNA were mixed at 0 mM phosphate, essentially all of the radiolabel could be pulled down, as expected (see groups 1 and 2 of Figure 6). This association was likely due to nonspecific binding of the radiolabeled 4WJ DNA to the peptide immobilized on the bead under conditions that also led to aggregation in the native gels (see Figure 2). The isolated globular domains of yeast Hho1p were previously shown to

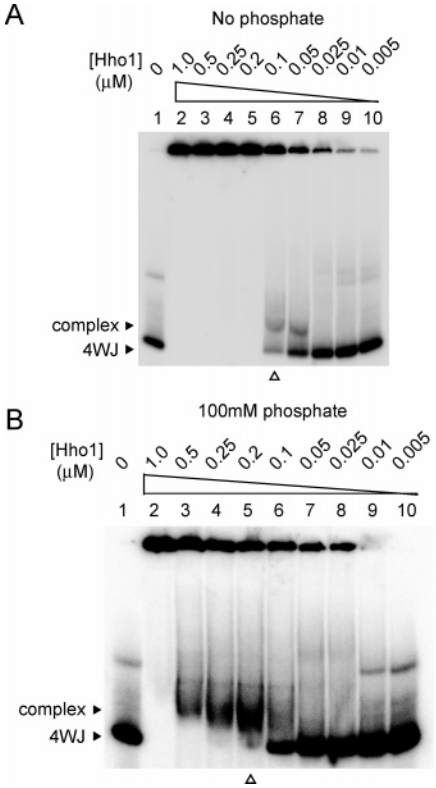

FIGURE 4: Binding of Hho1p to 4WJ DNA at different concentrations of sodium phosphate. The indicated amounts of full-length Hho1p (lanes 1−10) were incubated with 5 nM radiolabeled 4WJ DNA in the absence (A) or presence (B) of 100 mM sodium phosphate and electrophoretically resolved and visualized as in Figure 2. The positions of free 4WJ DNA, binary complexes, and lanes showing a 50% shift are indicated as in Figure 2.

bind to DNA−cellulose, which suggested nonspecific binding to duplex DNA (*26*). It was also shown that the single globular domain of chicken histone H1 or H5 simultaneously bound to two DNA duplexes (*35*) presumably due to the presence of two DNA binding sites (*12*), each composed of a cluster of basic amino acid residues (*9*). Since some of the amino acid residues forming the two DNA binding sites were conserved in both GD1 and GD2 (*11*), it was expected that these globular domains could similarly bind to the duplex DNA arm sections from two different 4WJ molecules, resulting in the observed nonspecific aggregation at high peptide concentrations.

The pelleting of the radiolabeled 4WJ observed in the pull-down assay was not due to nonspecific binding of the radiolabeled 4WJ directly to the streptavidin-coated bead but involved the immobilized protein, since little binding was observed at 0 mM phosphate in the absence of added globular domain peptide (group 3 in Figure 6). When either GD1 or GD2 and the 4WJ DNA were mixed at 100 mM phosphate, little radiolabel could be pelleted with GD1 (group 4, Figure 6), whereas slightly more radiolabel was pulled down with GD2 (group 5, Figure 6). This is in agreement with the higher apparent affinity of GD2 for 4WJ DNA observed in the native electrophoresis gels (Figure 3).

When the globular domain peptides were initially independently mixed at 100 mM phosphate with the beads, a condition under which only GD2 was expected to bind to the immobilized 4WJ (see Figure 3), followed by adding of the radiolabeled 4WJ DNA at 0 mM phosphate, where both

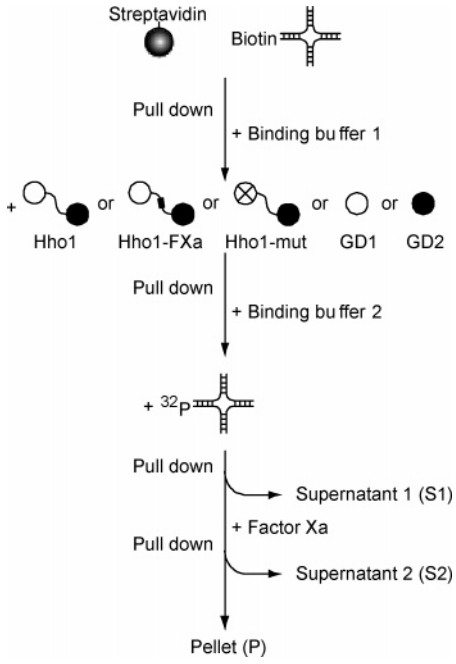

FIGURE 5: Bridged binding assay. Biotin-labeled 4WJ DNA was incubated with streptavidin-coated magnetic beads and equilibrated in binding buffer 1 containing sodium phosphate at the concentrations indicated in the text. The amounts of Hho1, Hho1-FXa, Hho1-mut, GD1, or GD2 indicated in the text were added, and after incubation, the beads were collected and transferred to binding buffer 2 containing the indicated sodium phosphate concentrations, and radiolabeled 4WJ DNA was added. The beads were again collected after incubation, and the distribution of the radiolabel between the supernatant (S1) and the bead (P) was determined by liquid scintillation counting. In some instances, the beads were transferred to factor Xa buffer and incubated with factor Xa before quantitation of the partitioning of the label between the supernatant (S2) and the bead.

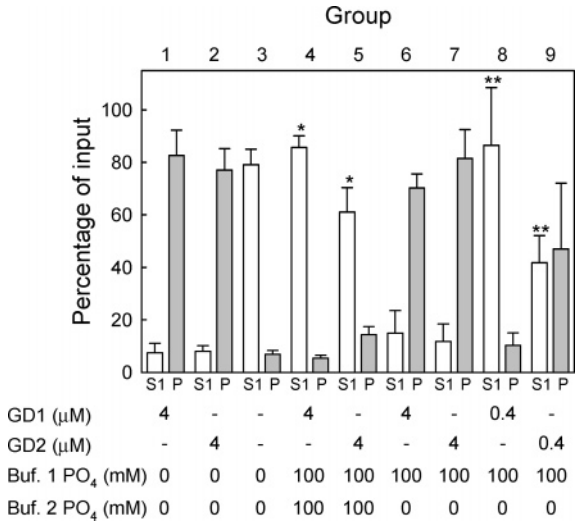

FIGURE 6: The bridged binding of GD1 and GD2 qualitatively mimics the electrophoretic mobility shift assay behavior. The partitioning of radiolabeled 4WJ DNA between the supernatant (S1) and pellet (P) was determined following binding of the indicated concentrations of GD1 (groups 1, 4, 6, and 8), GD2 (groups 2, 5, 7, and 9) or no peptide (group 3) to unlabeled 4WJ DNA immobilized on magnetic beads. The protein was added to the beads in buffer 1 containing 0 mM (groups 1−3) or 100 mM (groups 4−9) sodium phosphate and the radiolabeled 4WJ DNA in the presence of buffer 2, containing 0 mM (groups 1−3 and 6−9) or 100 mM (groups 4 and 5) sodium phosphate. The amount of radiolabel is shown as a percentage of the total amount of radiolabel that was retrieved. Recoveries that were statistically significantly different (Student's *t*-test) between two conditions are identified by single ($p < 0.05$) or double ($p < 0.01$) asterisks. Each column value represents the average of at least three independent determinations, and the error bars show the standard deviation at 3σ.

GD1 and GD2 were expected to bind, most of the radiolabel appeared in the pellet for both GD1 and GD2 (groups 6 and 7, Figure 6). The ability of GD1 to bind to the immobilized 4WJ DNA at 100 mM phosphate was most likely due to the high peptide concentration (4 μM), since higher peptide concentrations were found to result in aggregation in the electrophoresis assays (Figure 2). We therefore reduced the globular domain concentration to 0.4 μM, the highest peptide concentration where a clear binary complex and little aggregation were observed for the GD2 in the native gel assay (lane 7, Figure 2B). At this concentration, very little binding of the radiolabeled 4WJ to GD1 was observed (group 8, Figure 6). In contrast, a significant association was seen between GD2 and the radiolabeled 4WJ DNA ($p < 0.01$). This result demonstrated that the formation of the phosphate-dependent complexes observed by native gel electrophoresis could be qualitatively mimicked in the pull-down assay and also suggested that the binding of the two globular domains in Hho1p to 4WJ DNA could be regulated by adjustment of the phosphate concentration.

Hho1p Binds Specifically to 4WJ DNA. The binding behavior of recombinant full-length Hho1p was studied next in the pull-down assay using 0.1 μM protein, a concentration that resulted in a 50% shift in the native gel assay at 0 mM phosphate (lane 6, Figure 4A). When the binding assay was performed at 100 mM phosphate, where GD1 binds poorly, even at a peptide concentration of 4 μM (group 4 of Figure 6), significantly more radiolabeled 4WJ was pulled down by the full-length Hho1p molecule compared to either GD1 or GD2 alone (compare groups 4 and 5, Figure 6, to group 1, Figure 7A). This may have been due to the additional presence of the lysine-rich interglobular domain region in Hho1p, with may have contributed to stabilizing the binding of Hho1p to both the immobilized and the radiolabeled 4WJ DNA. The presence of the C-terminal tail of $H1^o$ was previously shown to increase the affinity of the peptide for 4WJ DNA relative to the globular domain alone (*31*). When the binding assay was performed at 0 mM phosphate, where GD1 was shown to bind to 4WJ DNA (lane 1, Figure 3, and group 6, Figure 6), a statistically significant ($p < 0.01$) increase in the amount of radiolabeled 4WJ that could be pulled down by full-length Hho1p was observed (compare groups 1 and 2, Figure 7A). This increase in binding under conditions where both globular domains can bind to 4WJ DNA suggested the involvement of both domains in the binding between the two 4WJ DNA molecules. In addition, this association appeared to be specific, where the Hho1p molecule recognized the molecular structure of the 4WJ, since there was a statistically significant ($p < 0.05$) decrease in binding when a radiolabeled double-stranded DNA oligomer was used instead of the 4WJ DNA (group 3, Figure 7A). Furthermore, substitution of the four conserved amino acid residues that formed the second DNA binding site of GD1 (*7*), a modification previously shown to abolish specific binding of the chicken H5 globular domain to nucleosome cores (*12*), resulted in a statistically significant ($p < 0.001$) decrease in binding of the mutant Hho1p protein to 4WJ DNA (compare groups 2 and 4, Figure 7A). Taken together,

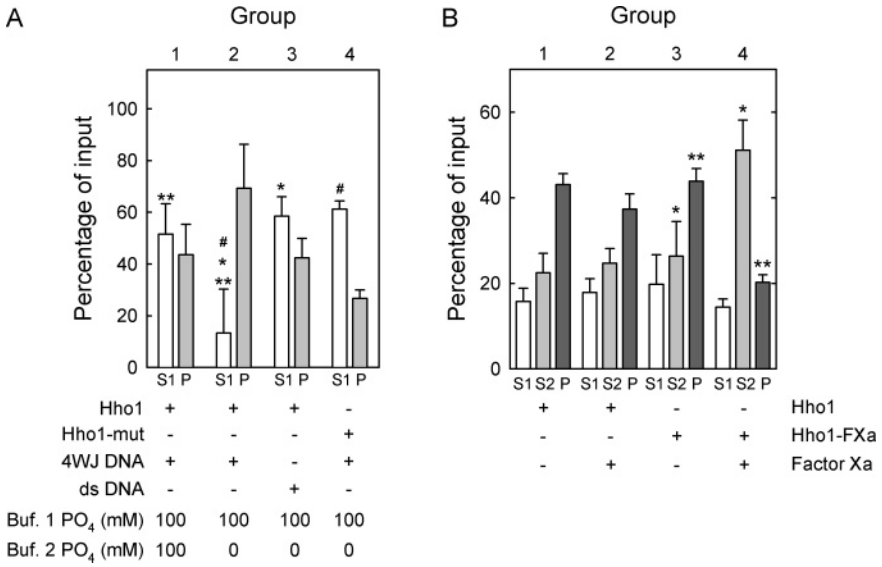

FIGURE 7: Hho1p simultaneously binds to two 4WJ DNA molecules in a structure-specific manner. (A) The partitioning of radiolabeled 4WJ DNA between the supernatant (S1) and pellet (P) was determined following binding of the indicated concentrations of Hho1 (groups 1−3) or Hho1-mut (group 4) to immobilized 4WJ DNA (groups 1, 2, and 4) or to duplex DNA (group 3). The radiolabeled 4WJ DNA was added in the presence of buffer 2 containing 0 mM (groups 2−4) or 100 mM (group 1) sodium phosphate. (B) The partitioning of radiolabeled 4WJ DNA between the pellet (P) and the supernatant before (S1) or after (S2) factor Xa cleavage was determined following Hho1 (groups 1 and 2) or Hho1-FXa (groups 3 and 4) incubation with unlabeled, immobilized 4WJ DNA and radiolabeled 4WJ DNA. Following removal of S1, buffer only (groups 1 and 3) or buffer containing factor Xa (groups 2 and 4) was added, and the amount of radiolabel released into the supernatant (S2), or remaining bound to the pellet (P), was determined. Percentages of the total amount of radiolabel recovered for every experimental condition are shown. Statistically significant differences in recovery are identified by asterisks as in Figure 6, and the octothorp indicates a statistically significant difference (Student's *t*-test) of $p < 0.001$. The column values represent the average of at least three independent determinations, and the error bars show the standard deviation at 3σ.

these results suggested that the full-length Hho1p bound to 4WJ molecules in a structure-specific manner that required both globular domains.

A Covalent Link between GD1 and GD2 Is Required for Bridged Binding between Two 4WJ Molecules. We next asked whether the observed binding to two 4WJ molecules involved the independent binding of both globular domains to different 4WJ molecules or simply the cross-binding of a single globular domain to two 4WJ molecules via the two DNA binding sites. To address this, we constructed a Hho1p molecule that contained a factor Xa site within the lysine-rich region between the two globular domains. The introduction of this four amino acid residue site did not change the net charge of the interglobular domain region. As expected, there was not a notable release of radiolabeled 4WJ DNA from the complexes pulled down in the presence of native Hho1p which lacked the factor Xa cleavage site, after treatment with factor Xa (compare groups 1 and 2, Figure 7B). This result showed that the incubation with the protease did not disrupt binding between Hho1p and the 4WJ DNA. In contrast, a significant increase ($p < 0.01$) in the amount of 4WJ released from the Hho1-FXa complex was observed following incubation with factor Xa (compare groups 3 and 4, Figure 7B). This result showed that retention of the radiolabeled 4WJ DNA on the bead required a covalent link between GD1 and GD2, suggesting that the two globular domains independently bound to two different 4WJ molecules.

DISCUSSION

We have shown that the yeast linker histone Hho1p can simultaneously bind to two 4WJ DNA molecules. This bridged binding required a covalent attachment between the globular domains, demonstrating that each globular domain was associated with a different 4WJ DNA. In addition, this binding was structure specific, since mutation of four conserved amino acid residues in DNA binding site 2 of GD1, previously shown to be required for the correct structural placement of the H5 globular domain in a nucleosome core (*12*), abolished the ability of Hho1p to bind in a bridged manner.

DNA Binding May Induce Folding in GD2. Several studies have reported that the purification of recombinant GD2 was technically problematic, probably due to the unfolded state of GD2 at lower ionic strengths (10 mM sodium phosphate) (*10*, *26*). Thomas and colleagues reported that GD2 only assumed an α-helical content comparable to that of GD1 in the presence of large tetrahedral anions (*7*, *26*). It is unlikely that the unfolded conformation of free GD2 at low ionic strengths has a major impact on the interpretation of our binding data. Notably, GD2 did bind to 4WJ DNA in the presence of 50 mM NaCl (*26*), a condition where the peptide was largely unstructured free in solution (*10*, *26*). This suggested that binding to DNA induced a structured conformation in GD2, similar to induction of a folded conformation in the C-terminal tail of H1 (*16*, *18*). The higher apparent affinity of GD2 for 4WJ DNA compared to that of GD1, a finding that was also reported by the Thomas laboratory (*26*), was contrary to expectation if GD2 existed in a largely unfolded conformation in the binding assay, since this would presumably have reduced the effective concentration of the peptide capable of binding to 4WJ DNA. We therefore expect that any effect of sodium or phosphate on the secondary and tertiary structure of GD2 was less significant than the induction of a folded conformation upon DNA binding.

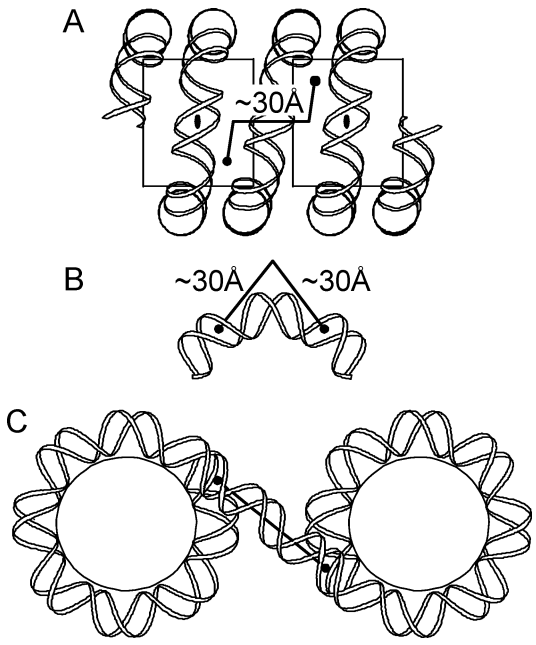

FIGURE 8: The length of peptide between GD1 and GD2 of Hho1p is sufficient to connect the two linker histone binding sites on adjacent nucleosomes. A schematic representation of two adjacent nucleosome cores showing the distance between the approximate positions of the globular domains (*3*) as a simple three-step function. The length of each segment in the step function is approximately 30 Å. (A) View from the side of DNA entry/exit. The number of helical periods per superhelical turn and the superhelix pitch angle were as reported (*2*, *40*) except for the terminal two-helical turns of each core, where a superhelix pitch angle of 10° was chosen to move the two cores slightly apart. (B) Part of the linker DNA connecting the two cores in (A), viewed along the superhelix axis. (C) Binding to adjacent nucleosome cores in a high-twist, two-start helix. A straight linker is shown, as was observed between the N2 and N2′ cores in the tetranucleosome crystal (*37*).

A Model for Binding to Two Nucleosome Cores Simultaneously. Both globular domains of yeast Hho1p (*6*, *11*) were shown to assume a single winged helix conformation (*7*, *10*). The basic amino acid residues in the two DNA binding sites were found to be conserved to differing degrees in both globular domains (*11*). Hho1p (*11*) and GD1 (*26*) caused a kinetic pause at 168 bp during MNase digestion. Furthermore, Hho1p formed a stable ternary complex with a dinucleosome (*11*), and we and others (*26*) have shown that Hho1p and both globular domains could bind with high affinity to 4WJ DNA. These results, taken together, suggested that both GD1 and GD2 recognized the DNA conformation at the point of DNA entry/exit in the nucleosome. In this study, we have shown that Hho1p could specifically and simultaneously bind to two different 4WJ molecules. This finding raised the possibility that one globular domain bound to one of two symmetrically related linker histone binding sites in one nucleosome core, allowing association of the lysine-rich interglobular domain of Hho1p with the linker DNA, and placing the second globular domain in the serially adjacent nucleosome. We were therefore interested in the structural implications of such an association and, in particular, whether the dimensions of the Hho1 protein allowed such bridged binding in chromatin.

In Figure 8A we show two nucleosome cores where the helical period of the two terminal turns of each core was altered to allow the proper setting of the pseudodyad axes. The crystal structure of the nucleosome core previously revealed that the terminal regions of DNA had the capacity to accommodate local twist changes (*2*). In addition, a superhelix angle of 10° was used for the terminal two helical turns to place approximately 5 Å between the neighboring octamers. The most inefficient path between the approximate positions of the globular domains (*3*) is a perpendicular step function of three segments. This function is composed of two segments that connect the position of either globular domain (Figure 8A) with a segment that is coaxial with the superhelix axis, located above the linker DNA (Figure 8B). The cumulative length of this step function is approximately 90 Å.

The C-terminal tail of H1 was shown to assume significant helicity in solution in the presence of large tetrahedral anions (*16*), and a considerable α-helical content was observed upon association with a DNA molecule (*17*, *18*). Similarly, the lysine-rich interglobular region of Hho1p also displayed an increase in helical content in the presence of a tetrahedral anion (*7*). These findings suggested that the interglobular region of Hho1p could assume an α-helical conformation when bound to the linker DNA. If the entire interglobular region between the C-terminal *β*-strand of GD1 and N-terminal α-helix of GD2 assumed the conformation of an α-helix, the axial length of the interglobular region would be 63×1.5 Å $= 95$ Å. This length is sufficient to connect the two linker histone binding sites on the two adjacent nucleosome cores using the very contorted step function path. This provides strong support to the idea that a shorter, optimized path can link the two GDs in neighboring nucleosomes. In addition, a longer length of peptide may be available to connect the two linker histone binding sites on the two nucleosomes, since the entire interglobular region may not become α-helical, due to the presence of helix-breaking residues, such as proline, in the sequence.

GD1 and GD2 May Be Present on the Same Nucleosome. Can GD1 and GD2 simultaneously bind to the two symmetrically related sites in a single nucleosome core, as is required by the repeated association of Hho1p to an array of nucleosomes in the manner proposed in Figure 8? Unlike GD1, GD2 did not confer a chromatosome stop to H1-stripped chromatin (*26*), which suggested that the binding mode of GD2 to a nucleosome may be different from that of GD1. In addition, only 50% of the residues that formed DNA binding site 2 in GD2 were conserved relative to chicken H5, compared to 100% in GD1. Significantly, GD2 lacked the equivalent of the K40 and R42 residues, located in the C-terminus of α-helix I and the unstructured region between α-helix I and II in the single winged helix fold (*7*, *9*). This part of the protein was shown to approach the DNA backbone enclosing the minor groove at the pseudodyad axis (*3*). The absence of these interactions to the central section of the nucleosome core may therefore allow the binding of GD2 to a nucleosome that already accommodated GD1 in the symmetrically related site on the same core. We note that GD2 was unstructured in solution and only assumed significant secondary structure in the presence of tetrahedral ions (*7*), and presumably DNA. This may indicate that GD1 targeted Hho1p to a nucleosome core and that GD2 only assumed a folded conformation once binding of the interglobular region had placed GD2 in the linker histone binding site of the adjacent nucleosome core. It is also possible that the two globular domains bind to the two linker histone

binding sites in the same nucleosome and that the lysine-rich interglobular region forms an extended hairpin loop that binds to and partially neutralizes the linker DNA.

Implications for a 30 nm Fiber in Yeast. The in vivo conformation of the 30 nm fiber remains unresolved, although there is substantial evidence for a two-start helical arrangement (*20*, *36*, *37*). Since nucleosomes from all studied metazoan chromatins possessed linker DNA (*38*), the need for the partial neutralization of the linker DNA in the condensed 30 nm fiber is evident (*39*). Even though the nucleosome repeat length in *S. cerevisiae* and neuronal cells is approximately 165 bp, this short length of linker DNA appears to be sufficient for the formation of a two-start helix (*37*). Steric clashes in the fiber center may be relieved by a radial translation of the nucleosome cores from the fiber axis. The slight structural disruption that this translation will cause may be accommodated by a movement of the H2A−H2B heterodimer in the core, as was suggested by the absence of stabilizing interactions in the H2A L1 loops where the H2A−H2B heterodimers interacted (*40*). It was also previously shown that yeast nucleosomal DNA was more permissive to thermal unwinding (*41*), suggesting that the terminal DNA−histone contacts may be more easily disrupted in yeast chromatin, facilitating formation of a two-start helix. The linear distance between the linker histone binding sites in a serially adjacent nucleosome pair in such a two-start helix is approximately 65 Å (Figure 8C). This strongly suggests that the *S. cerevisiae* Hho1p protein can, in principle, simultaneously bind to two nucleosome cores on opposite sides of a two-start chromatin fiber.

REFERENCES

1. Luger, K., Mader, A. W., Richmond, R. K., Sargent, D. F., and Richmond, T. J. (1997) Crystal structure of the nucleosome core particle at 2.8 Å resolution, *Nature 389*, 251−260.
2. Richmond, T. J., and Davey, C. A. (2003) The structure of DNA in the nucleosome core, *Nature 423*, 145−150.
3. Zhou, Y. B., Gerchman, S. E., Ramakrishnan, V., Travers, A., and Muyldermans, S. (1998) Position and orientation of the globular domain of linker histone H5 on the nucleosome, *Nature 395*, 402−405.
4. Parseghian, M. H., and Hamkalo, B. A. (2001) A compendium of the histone H1 family of somatic subtypes: an elusive cast of characters and their characteristics, *Biochem. Cell Biol. 79*, 289−304.
5. Wu, M., Allis, C. D., Sweet, M. T., Cook, R. G., Thatcher, T. H., and Gorovsky, M. A. (1994) Four distinct and unusual linker proteins in a mitotically dividing nucleus are derived from a 71-kilodalton polyprotein, lack p34cdc2 sites, and contain protein kinase A sites, *Mol. Cell. Biol. 14*, 10−20.
6. Landsman, D. (1996) Histone H1 in *Saccharomyces cerevisiae*: a double mystery solved?, *Trends Biochem. Sci. 21*, 287−288.
7. Ali, T., Coles, P., Stevens, T. J., Stott, K., and Thomas, J. O. (2004) Two homologous domains of similar structure but different stability in the yeast linker histone, Hho1p, *J. Mol. Biol. 338*, 139−148.
8. Cerf, C., Lippens, G., Ramakrishnan, V., Muyldermans, S., Segers, A., Wyns, L., Wodak, S. J., and Hallenga, K. (1994) Homo- and heteronuclear two-dimensional NMR studies of the globular domain of histone H1: full assignment, tertiary structure, and comparison with the globular domain of histone H5, *Biochemistry 33*, 11079−11086.
9. Ramakrishnan, V., Finch, J. T., Graziano, V., Lee, P. L., and Sweet, R. M. (1993) Crystal structure of globular domain of histone H5 and its implications for nucleosome binding, *Nature 362*, 219−223.
10. Ono, K., Kusano, O., Shimotakahara, S., Shimizu, M., Yamazaki, T., and Shindo, H. (2003) The linker histone homolog Hho1p from *Saccharomyces cerevisiae* represents a winged helix-turn-helix fold as determined by NMR spectroscopy, *Nucleic Acids Res. 31*, 7199−7207.
11. Patterton, H. G., Landel, C. C., Landsman, D., Peterson, C. L., and Simpson, R. T. (1998) The biochemical and phenotypic characterization of Hho1p, the putative linker histone H1 of *Saccharomyces cerevisiae*, *J. Biol. Chem. 273*, 7268−7276.
12. Goytisolo, F. A., Gerchman, S. E., Yu, X., Rees, C., Graziano, V., Ramakrishnan, V., and Thomas, J. O. (1996) Identification of two DNA-binding sites on the globular domain of histone H5, *EMBO J. 15*, 3421−3429.
13. Ponte, I., Vila, R., and Suau, P. (2003) Sequence complexity of histone H1 subtypes, *Mol. Biol. Evol. 20*, 371−380.
14. Suzuki, M. (1989) SPKK, a new nucleic acid-binding unit of protein found in histone, *EMBO J. 8*, 797−804.
15. Maeder, D. L., and Bohm, L. (1991) The C-domain in the H1 histone is structurally conserved, *Biochim. Biophys. Acta 1076*, 233−238.
16. Clark, D. J., Hill, C. S., Martin, S. R., and Thomas, J. O. (1988) Alpha-helix in the carboxy-terminal domains of histones H1 and H5, *EMBO J. 7*, 69−75.
17. Vila, R., Ponte, I., Collado, M., Arrondo, J. L., Jimenez, M. A., Rico, M., and Suau, P. (2001) DNA-induced alpha-helical structure in the NH_2-terminal domain of histone H1, *J. Biol. Chem. 276*, 46429−46435.
18. Vila, R., Ponte, I., Collado, M., Arrondo, J. L., and Suau, P. (2001) Induction of secondary structure in a COOH-terminal peptide of histone H1 by interaction with the DNA: an infrared spectroscopy study, *J. Biol. Chem. 276*, 30898−30903.
19. Thoma, F., Koller, T., and Klug, A. (1979) Involvement of histone H1 in the organization of the nucleosome and of the salt-dependent superstructures of chromatin, *J. Cell Biol. 83*, 403−427.
20. Dorigo, B., Schalch, T., Kulangara, A., Duda, S., Schroeder, R. R., and Richmond, T. J. (2004) Nucleosome arrays reveal the two-start organization of the chromatin fiber, *Science 306*, 1571−1573.
21. Graziano, V., Gerchman, S. E., Schneider, D. K., and Ramakrishnan, V. (1996) Neutron scattering studies on chromatin higher-order structure, *Basic Life Sci. 64*, 127−136.
22. Allan, J., Harborne, N., Rau, D. C., and Gould, H. (1982) Participation of core histone "tails" in the stabilization of the chromatin solenoid, *J. Cell Biol. 93*, 285−297.
23. Carruthers, L. M., and Hansen, J. C. (2000) The core histone N termini function independently of linker histones during chromatin condensation, *J. Biol. Chem. 275*, 37285−37290.
24. Dorigo, B., Schalch, T., Bystricky, K., and Richmond, T. J. (2003) Chromatin fiber folding: requirement for the histone H4 N-terminal tail, *J. Mol. Biol. 327*, 85−96.
25. Allan, J., Mitchell, T., Harborne, N., Bohm, L., and Crane-Robinson, C. (1986) Roles of H1 domains in determining higher order chromatin structure and H1 location, *J. Mol. Biol. 187*, 591−601.
26. Ali, T., and Thomas, J. O. (2004) Distinct properties of the two putative "globular domains" of the yeast linker histone, Hho1p, *J. Mol. Biol. 337*, 1123−1135.
27. Smith, J. A., Ausubel, F. M., Brent, R., Kingston, R. E., Moore, D. D., Struhl, K., and Seidman, J. G. (2002) Short protocols in molecular biology: A compendium of methods, in *Current Protocols in Molecular Biology*, John Wiley and Sons, New York.
28. Higuchi, R., Krummel, B., and Saiki, R. K. (1988) A general method of in vitro preparation and specific mutagenesis of DNA fragments: study of protein and DNA interactions, *Nucleic Acids Res. 16*, 7351−7367.
29. Boa, S., Coert, C., and Patterton, H. G. (2003) *Saccharomyces cerevisiae* Set1p is a methyltransferase specific for lysine 4 of histone H3 and is required for efficient gene expression, *Yeast 20*, 827−835.
30. Webb, M., and Thomas, J. O. (1999) Structure-specific binding of the two tandem HMG boxes of HMG1 to four-way junction DNA is mediated by the A domain, *J. Mol. Biol. 294*, 373−387.
31. Angelov, D., Novakov, E., Khochbin, S., and Dimitrov, S. (1999) Ultraviolet laser footprinting of histone H1(0)-four-way junction DNA complexes, *Biochemistry 38*, 11333−11339.

32. Varga-Weisz, P., Zlatanova, J., Leuba, S. H., Schroth, G. P., and van Holde, K. (1994) Binding of histones H1 and H5 and their globular domains to four-way junction DNA, *Proc. Natl. Acad. Sci. U.S.A 91*, 3525−3529.
33. Varga-Weisz, P., van Holde, K., and Zlatanova, J. (1993) Preferential binding of histone H1 to four-way helical junction DNA, *J. Biol. Chem. 268*, 20699−20700.
34. Joo, C., McKinney, S. A., Lilley, D. M., and Ha, T. (2004) Exploring rare conformational species and ionic effects in DNA Holliday junctions using single-molecule spectroscopy, *J. Mol. Biol. 341*, 739−751.
35. Thomas, J. O., Rees, C., and Finch, J. T. (1992) Cooperative binding of the globular domains of histones H1 and H5 to DNA, *Nucleic Acids Res. 20*, 187−194.
36. Woodcock, C. L., and Dimitrov, S. (2001) Higher-order structure of chromatin and chromosomes, *Curr. Opin. Genet. Dev. 11*, 130−135.
37. Schalch, T., Duda, S., Sargent, D. F., and Richmond, T. J. (2005) X-ray structure of a tetranucleosome and its implications for the chromatin fibre, *Nature 436*, 138−141.
38. Van Holde, K. D. (1989) *Chromatin*, Academic Press, New York.
39. Clark, D. J., and Kimura, T. (1990) Electrostatic mechanism of chromatin folding, *J. Mol. Biol. 211*, 883−896.
40. White, C. L., Suto, R. K., and Luger, K. (2001) Structure of the yeast nucleosome core particle reveals fundamental changes in internucleosome interactions, *EMBO J. 20*, 5207−5218.
41. Morse, R. H., Pederson, D. S., Dean, A., and Simpson, R. T. (1987) Yeast nucleosomes allow thermal untwisting of DNA, *Nucleic Acids Res. 15*, 10311−10330.

BI0511787